

A Light Harvesting Complex-Like Protein in Maintenance of Photosynthetic Components in *Chlamydomonas*¹[OPEN]

Lei Zhao,^a Dongmei Cheng,^{a,b} Xiahe Huang,^c Mei Chen,^a Luca Dall'Osto,^d Jiale Xing,^{a,b} Liyan Gao,^c Lingyu Li,^{a,b} Yale Wang,^{a,b} Roberto Bassi,^d Lianwei Peng,^{a,e} Yingchun Wang,^c Jean-David Rochaix,^f and Fang Huang^{a,2}

^aKey Laboratory of Photobiology, Institute of Botany, Chinese Academy of Sciences, Beijing 100093, China

^bUniversity of the Chinese Academy of Sciences, Beijing 100049, China

^cState Key Laboratory of Molecular Developmental Biology, Institute of Genetics and Developmental Biology, Chinese Academy of Sciences, Beijing 100101, China

^dDipartimento di Biotechnologie, Università di Verona, 37134 Verona, Italy

^eCollege of Life and Environmental Sciences, Shanghai Normal University, Shanghai 200234, China

^fDepartments of Molecular Biology and Plant Biology, University of Geneva, 1211 Geneva, Switzerland

ORCID IDs: 0000-0001-9497-5156 (L.D.); 0000-0002-4140-8446 (R.B.); 0000-0001-8483-777X (J.-D.R.); 0000-0001-8963-447X (F.H.).

Using a genetic approach, we have identified and characterized a novel protein, named Msf1 (Maintenance factor for photosystem I), that is required for the maintenance of specific components of the photosynthetic apparatus in the green alga *Chlamydomonas reinhardtii*. Msf1 belongs to the superfamily of light-harvesting complex proteins with three transmembrane domains and consensus chlorophyll-binding sites. Loss of Msf1 leads to reduced accumulation of photosystem I and chlorophyll-binding proteins/complexes. Msf1 is a component of a thylakoid complex containing key enzymes of the tetrapyrrole biosynthetic pathway, thus revealing a possible link between Msf1 and chlorophyll biosynthesis. Protein interaction assays and greening experiments demonstrate that Msf1 interacts with Copper target homolog1 (CHL27B) and accumulates concomitantly with chlorophyll in *Chlamydomonas*, implying that chlorophyll stabilizes Msf1. Contrary to other light-harvesting complex-like genes, the expression of *Msf1* is not stimulated by high-light stress, but its protein level increases significantly under heat shock, iron and copper limitation, as well as in stationary cells. Based on these results, we propose that Msf1 is required for the maintenance of photosystem I and specific protein-chlorophyll complexes especially under certain stress conditions.

The major role of the photosynthetic apparatus is to capture light excitation energy and to convert it into chemical energy. In photosynthetic eukaryotes, light is absorbed by the light-harvesting complexes (LHC) of

PSII and PSI and transferred to the corresponding reaction centers, which act in series in photosynthetic electron transport. These processes induce stable charge separations across the thylakoid membrane and generate electron flow from water to NADP⁺, leading to the production of energy and reducing power (ATP and NADPH) for CO₂ fixation. PSI is a multiprotein complex acting as a light-driven plastocyanin-ferredoxin oxidoreductase, ultimately leading to the reduction of NADP⁺ into NADPH. The PSI core is surrounded by LHCI, forming a PSI-LHCI complex, to facilitate efficient light harvesting (Scholes et al., 2011). The energy absorbed by LHCI is transferred to the PSI core, where it induces charge separation across the thylakoid membrane with nearly 100% efficiency (Nelson, 2009). How this large chlorophyll-protein complex is assembled and how its photosynthetic activity is maintained under various stress conditions remain open questions (Amunts and Nelson, 2009).

Recent advances in structural biology have resolved the crystal structure of the PSI-LHCI complex from higher plants at 2.8 Å resolution (Mazor et al., 2015; Qin et al., 2015). The complex contains at least 16 core subunits and four LHCI proteins (Lhcas) as well as a

¹ This study was supported by grants from the Ministry of Science and Technology of China (grant no. 2015CB150100); the National Natural Science Foundation of China (grant nos. 31270288 and 31470340 to F.H. and grant no. 31400212 to M.C.); the Strategic Priority Research Program (grant no. XDB17030100) and the Foreign Expert Program (to J.-D.R.) of the Chinese Academy of Sciences; and the Marie Curie Actions Initial Training Networks ACCLIPHOT (grant no. PITN-GA-2012-316427).

² Address correspondence to fhuang@ibcas.ac.cn.

The author responsible for distribution of materials integral to the findings presented in this article in accordance with the policy described in the Instructions for Authors (www.plantphysiol.org) is: Fang Huang (fhuang@ibcas.ac.cn).

L.Z., J.-D.R., and F.H. designed the experiments, discussed/analyzed data, and wrote the article; L.Z., D.C., M.C., J.X., Y.W., and L.P. performed the genetic and biochemical assays; Y.W., X.H., and L.G. carried out the mass spectrometry analysis; R.B. and L.D. carried out the pigment reconstitution experiments; L.Z. carried out all other experiments described in this article; F.H. and J.-D.R. supervised the project.

[OPEN] Articles can be viewed without a subscription.

www.plantphysiol.org/cgi/doi/10.1104/pp.16.01465

large number of cofactors, including 155 chlorophylls and 35 carotenoids. A belt of Lhca subunits is located on one side of the PSI core, with several specific interaction sites between the PSI core and LHCI.

LHC-like proteins are distant relatives of the common light-harvesting chlorophyll a/b-binding proteins in higher plants and green algae. These proteins contain up to four transmembrane domains with conserved chlorophyll-binding sites and have been identified in land plants and green algae (Teramoto et al., 2004, 2006; Beck et al., 2017) as well as in cyanobacteria (Kufryk et al., 2008; Cheregi et al., 2012; Staleva et al., 2015; Komenda and Sobotka, 2016). They include the one-helix proteins (OHPs), also named HLIPs (high-light-induced proteins), two-helix stress-enhanced proteins (SEPs), three-helix early light-induced proteins (ELIPs; for review, see Heddad and Adamska, 2002; Komenda and Sobotka, 2016), and the four-helix PsbS protein that is unable to bind pigments (Kim et al., 1992). Although these proteins contain similar LHC motifs in their sequences, the individual roles of these proteins appear to be distinct. For example, the three-helix LHC-like proteins are diversified mainly as LhcSRs and ELIPs for photoprotection. The former proteins are involved specifically in dissipating excess energy through nonphotochemical quenching (Niyogi and Truong, 2013), whereas the ELIPs are expressed almost exclusively under light stress or during deetiolation of proplastids and are assumed to play a protective role in high light by scavenging free chlorophylls, or by assisting the assembly and stabilization of photosynthetic pigment-protein complexes, and/or by acting as pigment carriers during assembly or by regulating chlorophyll metabolism (Montané and Kloppstech, 2000; Adamska, 2001; Heddad and Adamska, 2002; Hutin et al., 2003; Elrad and Grossman, 2004; Tzvetkova-Chevolleau et al., 2007). Compared with the intensive studies, both in vivo and in vitro, aimed at elucidating the specific roles of individual LhcSR proteins during the quenching process (Niyogi and Truong, 2013; Dinc et al., 2016), detailed characterization of other LHC-like proteins with three transmembrane domains is still scarce, probably due to their low abundance. Their precise role, therefore, is still largely unknown. In cyanobacteria, HLIPs play important roles as carriers of newly synthesized pigments during the assembly of PSII and potentially also PSI (Chidgey et al., 2014; Knoppová et al., 2014; Akulinkina et al., 2015; Komenda and Sobotka, 2016). These proteins were identified by their increased expression during high-light stress, when photodamaged photosystems have to be degraded and replaced. In this process, HLIPs also may be involved in the recycling of pigments from damaged photosystems or antennae (Dolganov et al., 1995; Havaux et al., 2003). Additionally, these proteins may be involved in the regulation of tetrapyrrole biosynthesis in response to pigment availability (Xu et al., 2002, 2004).

Here, we have identified and characterized a novel protein, named Msf1 (Maintenance factor for photosystem I), an LHC-like protein with three transmembrane domains in the green alga *Chlamydomonas reinhardtii*

(henceforth referred to as *Chlamydomonas*). This factor is required mainly for the stability and maintenance of PSI. It appears to interact with enzymes of the tetrapyrrole pathway, and its abundance increases under specific stress conditions and in aging cells. We propose that Msf1 is a potential candidate to link chlorophyll synthesis with the maintenance of chlorophyll-binding protein complexes, in particular PSI, under certain stress conditions.

RESULTS

The *msf1* Mutant Is Impaired in Photosynthetic Activity

The *msf1* mutant was isolated during a genetic screen for *Chlamydomonas* mutants with reduced photosynthetic activity. Figure 1 shows that the growth of *msf1* both in liquid medium (Fig. 1A; TAP) and on agar plates containing high salt medium (Fig. 1B; HSM) was decreased compared with the wild type, suggesting reduced oxygenic photosynthesis in the mutant. This was indeed the case, as shown by the light-response curves based on chlorophyll fluorescence measurements (Imaging PAM; Heinz Walz), indicating that the effective photochemical quantum yield of PSII (Φ_{II}) of *msf1* is significantly lower than that of the wild type (Fig. 1C). Further analysis of photosynthetic pigments by HPLC showed that the pigment content ($\mu\text{g cell}^{-1}$) decreased nearly 50% in the mutant. To test whether the significant change in pigment content in *msf1* was accompanied by alterations in chloroplast ultrastructure, transmission electron microscopy was performed. This analysis indeed showed that, in comparison with the wild type, thylakoid membrane organization was altered (Supplemental Fig. S2A). In the wild type, these membranes were appressed, with two or more layers of grana stacks in most cases, whereas in *msf1*, the proportion of single-layer thylakoid membranes was significantly higher, indicating that thylakoid stacking is affected in the mutant (Supplemental Fig. S2B). We also found that the cell size of *msf1* was larger than that of the wild type (Supplemental Fig. S2C), while the protein content was comparable (Table I).

The Accumulation and Stability of PSI Is Affected in *msf1*

To investigate whether PSI is affected in *msf1*, low-temperature fluorescence (77K) emission spectra of wild-type and mutant cells were compared. Clearly, the maximal fluorescence emission peak at 717 nm in the wild type, characteristic for a functional PSI in green algae, was shifted to 711 nm in *msf1* (Fig. 1D). Similar observations have been reported in well-characterized PSI mutants from *Chlamydomonas* (Wollman and Bennoun, 1982). In these mutants, the partial loss of the PSI core complex leads to the release of some Lhcl antenna that gives rise to high fluorescence in the 705- to 710-nm region (Wollman and Bennoun, 1982; Takahashi et al., 2004).

To test whether the accumulation of PSI is affected in *msf1*, we compared the levels of several key proteins of the photosynthetic apparatus by immunoblot analysis

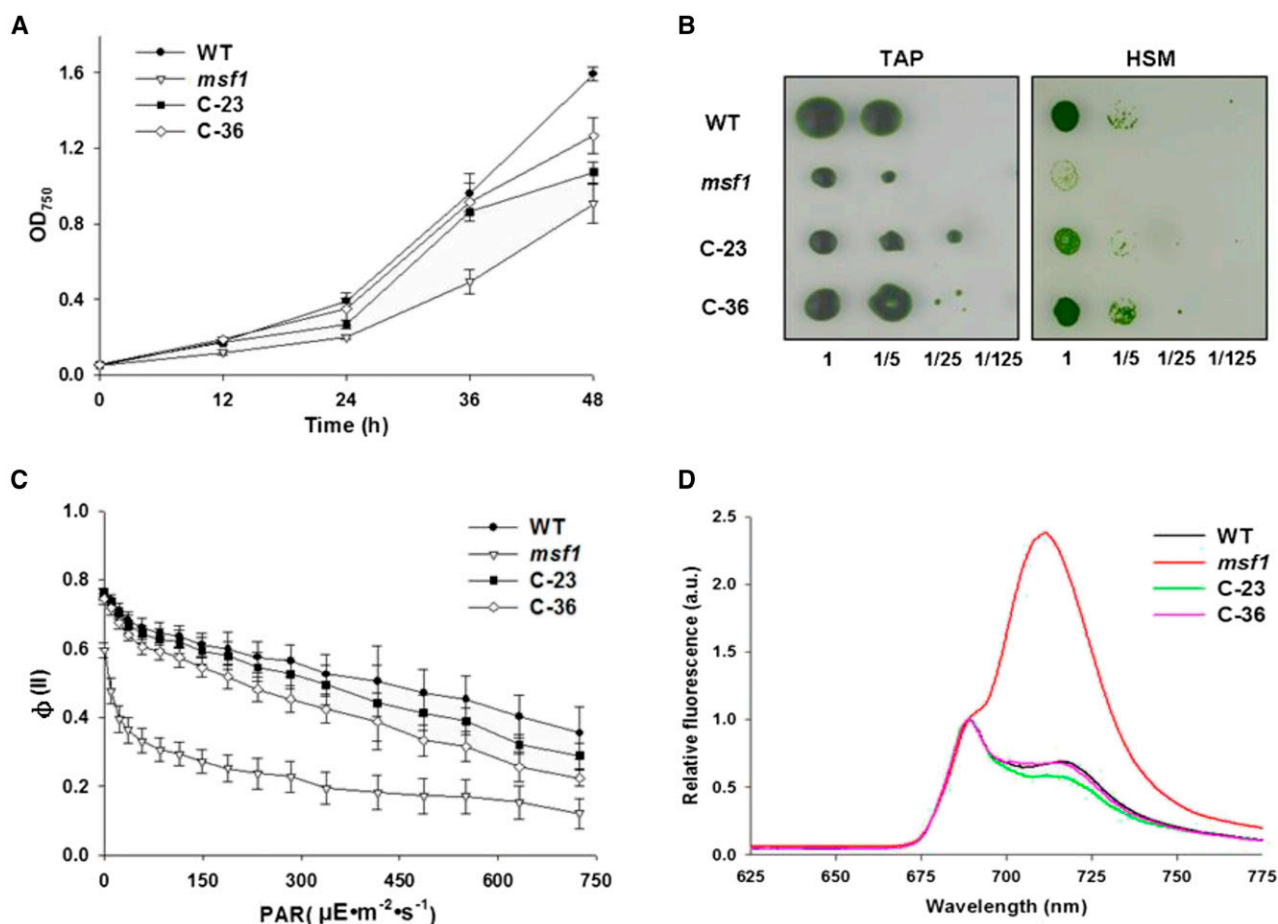


Figure 1. Growth and photosynthetic characteristics of the wild type (WT), *msf1*, and the complemented strains (C-23 and C-36). A and B, Growth profiles in liquid medium (Tris-acetate phosphate [TAP]; A) and on agar plates (B) with an irradiance of $60 \mu\text{mol photons m}^{-2} \text{s}^{-1}$. In A, sd values were estimated from three biological replicates each with three technical replicates. In B, cells with 5-fold serial dilutions (from 2 to 4×10^6 cells mL^{-1}) were spotted on plates and grown for 4 d (TAP) and 8 d (high salt medium [HSM]). C, Plots of Φ_{II} versus photosynthetically active radiation (PAR) of the indicated strains. sd values were estimated from three biological replicates each with three technical replicates. D, 77K fluorescence emission spectra of the indicated strains. The spectra were normalized with the GFP fluorescence peak at 513 nm according to Pinnola et al. (2015). The experiment was repeated more than three times with similar results.

(Fig. 2A). The levels of reaction center proteins (PsaA, PsaB, and PsaC) and of the peripheral subunits (PsaD and PsaF) of PSI in *msf1* were 25% or less that in the wild type. Also, the levels of some PSI antenna proteins were undetectable (Lhca7 and Lhca8), while those of other Lhca proteins (Lhca1, Lhca3, Lhca4, Lhca5, Lhca6, and Lhca9) as well as of the core subunits of PSII (D1, D2, CP43, and CP47), cytochrome *b₆f* (Cytb₆f), and ATP synthase (AtpB) were, to a large extent, unchanged or diminished in *msf1*. We also noticed that the levels of LHCII proteins (i.e. LhcII and CP29) were reduced (Fig. 2). These results indicate that the accumulation of PSI and of a restricted set of chlorophyll-binding proteins is affected in *msf1*. Moreover among the PSI assembly factors, the amount of Ycf3 was reduced while no decrease of Ycf4 was observed (Fig. 2).

Because the levels of the core subunits of PSII were not changed whereas those of the PSI subunits and some of its antenna proteins were reduced significantly (Fig. 2), we conclude that the stability of PSI is preferentially affected,

leading to reduced PSI activity in *msf1* (Fig. 1D). To further verify this point, we performed experiments with translation inhibitors and determined the quantity of several core subunits of PSI (PsaA and PsaD) and PSII (D1; Fig. 3). In the presence of chloramphenicol, a specific inhibitor of chloroplast translation, the decrease of PsaA, but not of D1, was significantly higher in *msf1* than in the wild type. A similar trend was observed for PsaD in the presence of cycloheximide, which inhibits the translation of cytosolic proteins (Fig. 3). These results clearly show that PSI is less stable in *msf1*.

The *msf1* Mutant Is Deficient in an LHC-Like Protein

DNA-blot analysis revealed that the *msf1* mutant contains a single insertion of the paromomycin resistance cassette in its nuclear genome (Supplemental Fig. S1A). The insertion site was mapped on the *Chlamydomonas* genome by sequencing the flanking regions of the

Table I. Pigment and protein content in the wild type (CC400), *msf1*, and the complemented strains (C-23 and C-36)

Values represent means \pm SE of three biological replicates each with two technical replicates. Protein content was estimated from cells in exponential growth according to Bradford (1976) using BSA as a standard. Chla, Chlorophyll *a*; Chlb, chlorophyll *b*; Neo, neoxanthin; Viola, violaxanthin; Anthera, antheraxanthin; Lut, Lutein; α -Car, α -carotene.

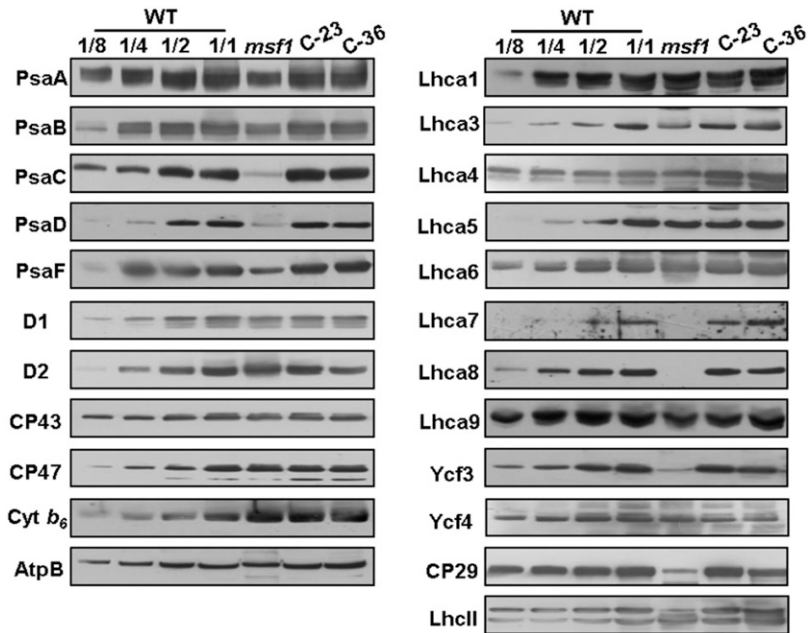
Strain	Chla	Chlb	Neo	Viola	Anthera	Lut	α -Car	Protein
Wild type	33.13 \pm 3.08	12.82 \pm 1.77	8.19 \pm 0.70	6.22 \pm 0.65	0.44 \pm 0.08	4.57 \pm 0.26	4.45 \pm 0.74	20.5 \pm 4.0
<i>msf1</i>	16.92 \pm 2.82	6.16 \pm 0.91	4.10 \pm 0.85	3.67 \pm 0.36	0.29 \pm 0.05	2.43 \pm 0.28	1.38 \pm 0.19	18.1 \pm 3.3
C-23	27.30 \pm 3.79	10.60 \pm 1.62	7.25 \pm 0.96	5.53 \pm 0.90	0.44 \pm 0.08	4.25 \pm 0.61	4.25 \pm 0.79	20.9 \pm 2.9
C-36	32.99 \pm 4.56	12.32 \pm 0.73	9.39 \pm 1.73	7.04 \pm 1.37	0.56 \pm 0.15	5.73 \pm 0.66	5.34 \pm 1.02	20.7 \pm 3.4

insert through thermal asymmetric interlaced PCR (Liu and Chen, 2007). Analysis of this genomic region in *msf1* revealed a DNA rearrangement resulting in the deletion of two genes, Cre14.g626750 and Cre14.g626800 (Supplemental Fig. S1B). The *msf1* mutant phenotype could only be rescued by transformation with Cre14.g626750 based on growth patterns and Φ II values (Supplemental Fig. S1C). Analysis of genetic crosses between *msf1* and the wild type was in agreement with these data (Supplemental Fig. S1E). The photosynthesis-deficient phenotype of *msf1* cosegregated with paromomycin resistance in several tetrads, suggesting that the phenotype is linked to this genetic disruption. This was confirmed by introducing a wild-type copy of the Cre14.g626750 gene into *msf1* (Supplemental Fig. S1D). Immunoblot analysis revealed that, in most transformants, the amount of PSI was restored to wild-type levels, indicating that the loss of this gene is responsible for the deficiency in PSI. Two of the complemented strains (i.e. C-23 and C-36) were analyzed further. Their 77K fluorescence emission spectra (Fig. 1D) were restored as in the wild type, as well as the levels of chlorophyll (Table I) and the organization of thylakoid membranes (Supplemental Fig. S2). Based on these experimental results, we conclude that

disruption of the Cre14.g626750 gene is the cause of the observed photosynthetic deficiency of the *msf1* mutant.

Sequence analysis revealed that Cre14.g626750 encodes a protein consisting of 192 amino acids with a putative transit peptide and three transmembrane domains with four chlorophyll-binding sites related to the light-harvesting system (Fig. 4A). A BLAST search indicated that the proteins with more than 30% sequence identity are present in algae, including *Volvox carteri* and *Chlorella variabilis*, as well as in higher plants, such as wheat (*Triticum aestivum*) and rice (*Oryza sativa*). These proteins are annotated as carotene biosynthesis-related or putative ELIPs (Heddad and Adamska, 2002). Indeed, an ELIP consensus sequence, ERINGRLAMIGFVAALAVE (Heddad and Adamska, 2002), is present in Msf1 (Fig. 4A). A sequence alignment of Msf1 versus two of the *Chlamydomonas* Lhcb sequences (Lhcbm1 and CP26) and one ELIP (ELI1) from *Chlamydomonas* and one ELIP (AtELIP1) from *Arabidopsis* (*Arabidopsis thaliana*) allowed us to determine the residues involved in chlorophyll *a* (A sites) and chlorophyll *b* (B sites) binding in Msf1 (Fig. 4A). Two ionic E-R pairs at the A4 and A1 sites (i.e. E87-R171 and E166-R92, respectively) are conserved. The side chains of these Glu residues (E) are close to charge-compensating Arg (R),

Figure 2. Abundance of photosynthetic subunits in the wild type (WT), *msf1*, and the complemented strains (C-23 and C-36). Total protein (15 μ g per lane) was separated by 12% SDS-PAGE followed by immunoblot detection of the indicated proteins. A dilution series of wild-type protein extract was used to quantify the amount of proteins in *msf1*. Similar results were obtained in at least three independent experiments.



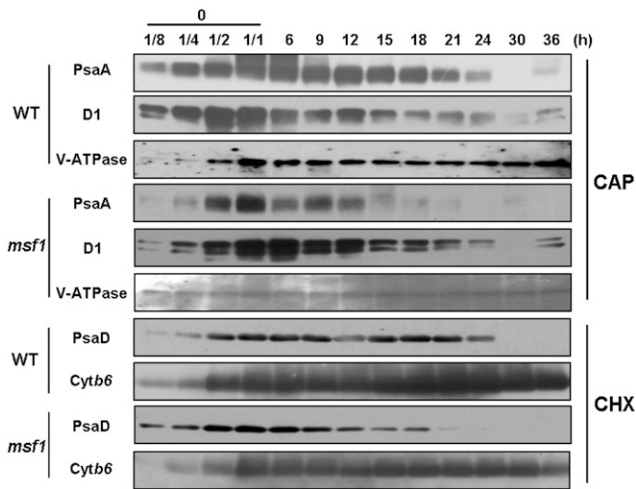


Figure 3. Immunoblot analysis of PSI and PSII proteins (PsaA, PsaD, and D1) from wild-type (WT) and *msf1* cells upon inhibition of translation in the chloroplast and cytosol with chloramphenicol (CAP; 100 $\mu\text{g mL}^{-1}$) and cycloheximide (CHX; 10 $\mu\text{g mL}^{-1}$). Total protein extracted from wild-type and *msf1* cells sampled at 10 time points (from 0 to 36 h) was separated by 12% SDS-PAGE (20 μg per lane) followed by immunoblot detection. V-ATPase and Cytb₆f were used as loading controls, respectively. Four serial dilutions of the protein extracts were used to quantify the immunosignals of the indicated proteins. Similar results were obtained in at least three independent experiments.

which are conserved in LHC proteins and responsible for the crossed arrangement of the first and third LHC helices (Kühlbrandt et al., 1994). The ligand for A5 in Msf1 is Asn (N90) instead of His and that of A2 is His (H169) rather than Asn. Other residues for chlorophyll-binding sites (A3, B3, B5, and B6) and the Tyr residue of the neoxanthin-binding site (N1; Caffarri et al., 2007) are not conserved (Fig. 4A).

To estimate the abundance of Msf1, we expressed recombinant Msf1 protein in *Escherichia coli* and generated an antibody followed by immunoblotting using protein extracts from the wild type. However, the protein was undetectable (Supplemental Fig. S3B), presumably due to its low accumulation and/or the low sensitivity of the antibody. This sensitivity was determined using serial dilutions of recombinant Msf1 until it was undetectable by immunoblotting. The limit of detection was 3 ng in an extract of 20 μg of total protein. This would correspond to 10^5 copies of Msf1 per cell, which presumably vastly exceeds the actual number (Supplemental Fig. S3, A and B; for details, see Supplemental Data Set S1). In order to be able to detect Msf1, we fused its cDNA to GFP driven by the *PsaD* promoter and introduced this construct by transformation in the UVM4 strain designed for increased expression of transgenes (Neupert et al., 2009). The detection limit for the Msf1-GFP with GFP antibody was around 0.012 ng. The level of Msf1 in numerous transformants, including the Msf1-GFP14 and Msf1-GFP16 strains, was then examined by immunoblotting with GFP antibody (Beijing TransGen Biotech). Clearly, a protein of approximately 47 kD, the expected size for

Msf1-GFP, was detected in the transformants, while no signal was detected in the nontransformed UVM4 strain (Fig. 4B), indicating that the transformed strains and GFP antibody could be used for the quantification of Msf1. Using the previously published protocol (Rahire et al., 2012), the number of Msf1 molecules in Msf1-GFP16 (Supplemental Fig. S3C) was estimated at 200 per cell.

As Msf1 is predicted to be an LHC-like protein, it was of interest to assess its chlorophyll-binding properties. Accordingly, we performed in vitro reconstitution experiments with the recombinant Msf1 protein using a published protocol that has been used successfully in similar circumstances (Cammarata et al., 1992; Dominici et al., 2002; Bonente et al., 2008, 2011). However, in spite of several trials, the results of these experiments were inconclusive (data not shown), presumably because the binding of chlorophyll to Msf1 is weak. We also tested whether the Msf1-GFP fusion protein is functional by transforming the *msf1* mutant with the corresponding gene construct driven by the authentic Msf1 promoter. Expression of the chimeric gene was verified by qRT-PCR analysis in two of the transformants, C6 and C25 (Supplemental Fig. S4). However, the expression of the protein was too low to be detected by immunoblotting with GFP antibodies. Further analysis revealed that the wild-type values of the photosynthetic parameters F_v/F_m and Φ_{II} were partially restored. Similarly, the low-temperature (77K) fluorescence emission spectra of C6 and C25 were intermediate between those of the wild type and *msf1*. Taken together, these results suggest that Msf1-GFP is at least partially functional in vivo.

Since LHC-like genes are known to be associated with light stress responses, we examined the expression profile of Msf1 in response to high-light stress ($1,300 \mu\text{mol photons m}^{-2} \text{s}^{-1}$) by qRT-PCR using total mRNA isolated from wild-type cells collected at different time points of the treatment (Supplemental Fig. S5). Because LhcSR3.1 and ELIP2-1 also are LHC-like proteins and their gene expression in response to high-light stress has been reported (Elrad and Grossman, 2004; Peers et al., 2009), we purposely used *LhcSR3.1* and *ELI2-1* as positive and negative controls in these experiments. Contrary to expectation based on studies of *LhcSR3.1*, no increase in the level of Msf1 transcript was detected during 60 min of high-light treatment (Supplemental Fig. S5).

Msf1 Interacts with at Least One Component of the Chlorophyll Biosynthesis Pathway

To determine whether Msf1 is associated with a thylakoid membrane complex, we analyzed membrane fractions of the wild type (UVM4), the Msf1-GFP strains (Msf1-GFP14 and Msf1-GFP16), and *msf1* by 2D blue-native (BN)/SDS-PAGE using a slightly modified protocol (Yang et al., 2014). The UVM4 strain was used in order to increase the expression of the chimeric Msf1-GFP protein. Solubilized membranes were separated

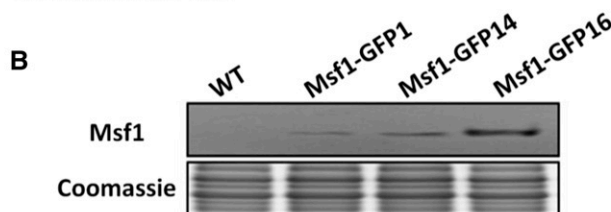
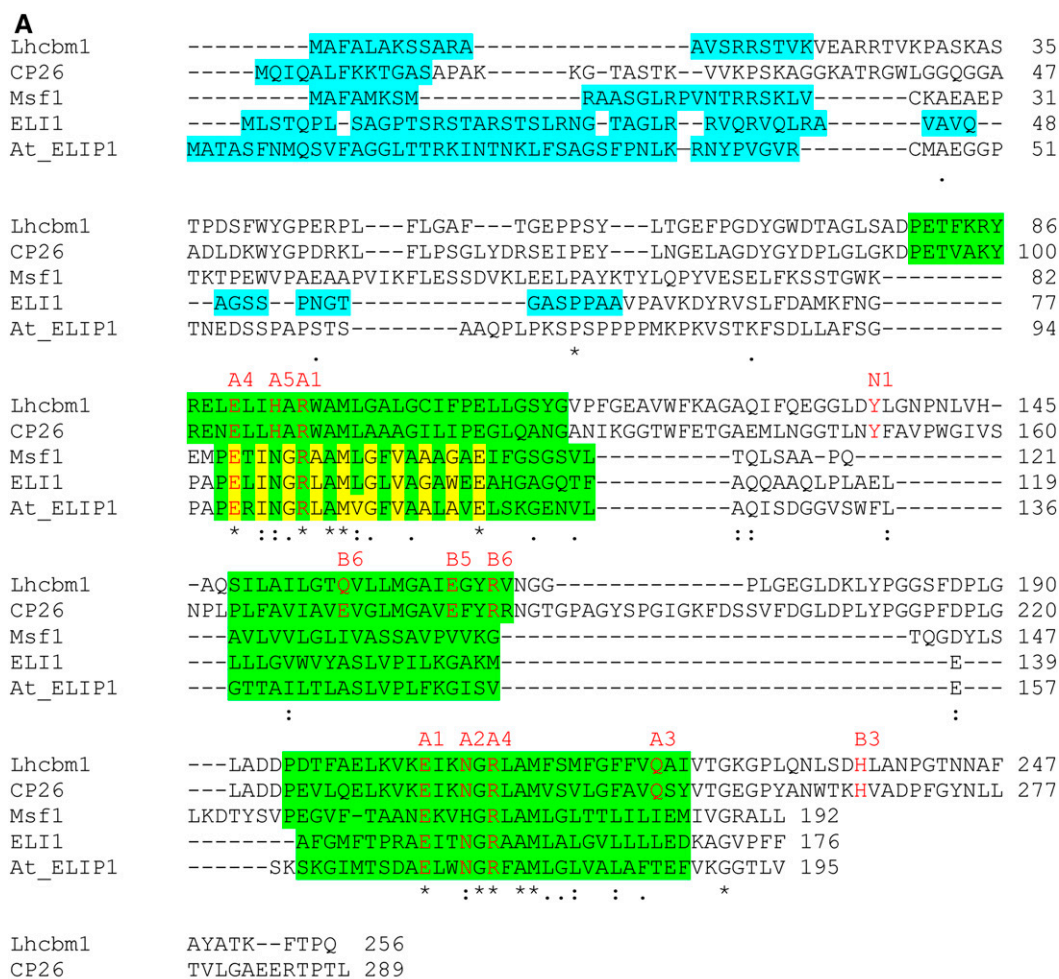


Figure 4. Sequence analysis and abundance of Msf1 in *Chlamydomonas*. A, Comparison of sequences of Msf1, Lhcbm1, CP26, and ELI1, from *Chlamydomonas* and ELIP1 from *Arabidopsis*. ChloroP (<http://www.cbs.dtu.dk/services/ChloroP/>) and Predalgo were used for the prediction of the transit peptides. The indicated transmembrane domains were based on the atomic structure of LHCII (Kühlbrandt et al., 1994). The transit peptides and three transmembrane domains are highlighted in blue and green, respectively. Pigment-binding sites are indicated in red: A1 to A5, B3 to B6, and N1 refer to chlorophyll *a*-, chlorophyll *b*-, and neoxanthin-binding sites, respectively. The ELIP consensus sequence in Msf1 is underlined. Asterisks, colons, and periods show identical, strongly similar, and weakly similar residues, respectively. Gaps introduced to optimize sequence alignment are indicated with dashes. B, Msf1 protein levels in the wild type (WT; UVM4) and three independent transformants (Msf1-GFP1, Msf1-GFP14, and Msf1-GFP16) quantified by immunoblotting against GFP antibody. Total protein (20 μ g per lane) was separated by 12% SDS-PAGE. Similar results were obtained in at least three independent experiments.

using BN-PAGE in the first dimension, then resolved with denaturing SDS-PAGE in the second dimension, followed by immunodetection with specific antibodies (Fig. 5). The immunosignal of GFP in the Msf1-GFP strains could only be detected in the spot corresponding to a complex of approximately 150 kD, indicating that Msf1 was associated with this complex. Interestingly, trace amounts of

PsaA also were detected in this complex, while the majority of PsaA was associated with larger complexes, as expected.

To identify proteins cofractionated with Msf1 in the complex, the gel band corresponding to the complex in the respective strains was excised and subjected to liquid chromatography-tandem mass spectrometry

(LC-MS/MS) analysis using a protocol optimized based on previous studies (Wang et al., 2000; Huang et al., 2002; Fandiño et al., 2005; for details, see “Materials and Methods”). Only proteins present either in the wild type or Msf1-GFP strains but absent in the *msf1* mutant were considered to be putative components of the complex. In further analysis of the proteins using the PredAlgo (<https://giavap-genomes.ibpc.fr/cgi-bin/predalgotdb.perl?page=main>) and TMHMM version 2 (<http://www.cbs.dtu.dk/services/TMHMM/>) prediction programs, only known photosynthetic proteins and proteins predicted to be localized in the chloroplast with transmembrane domain(s) were included (Supplemental Table S1). This set of proteins comprises several subunits of the photosynthetic apparatus and low-CO₂-inducible proteins as well as Cth1 (Copper target homolog1; CHL27B) and Cgl78/Ycf54. Both of the latter two proteins are involved in the chlorophyll biosynthetic pathway. Cth1 is a subunit of the chlorophyll cyclase that catalyzes the conversion of Mg-protoporphyrin IX monomethylester into divinyl protochlorophyllide, and Cgl78/Ycf54 regulates the activity of the chlorophyll cyclase (Moseley et al., 2002b; Tottey et al., 2003; Hsieh et al., 2013). The presence of Msf1 and these two proteins in the same complex (Fig. 5; Supplemental Table S1) suggests an association of these proteins. To test this possibility, split ubiquitin-based yeast two-hybrid (Y2H) assays were performed (Fig. 6A). The results show that Msf1 interacts with Cth1 (NubG-Cth1 and Cth1-NubG) but that no interaction with Cgl78/Ycf54 was detected, indicating that Msf1 interacts directly with at least one of the components of the chlorophyll biosynthetic pathway. Thus, a possible link between chlorophyll synthesis and the maintenance of pigment-protein complexes mediated through Msf1 may exist.

To further clarify that Msf1 is connected to chlorophyll synthesis via Cth1, we compared the mRNA and

protein levels of Cth1 in the wild type, *msf1*, and two complemented strains (Fig. 6, B and C). Interestingly, both transcript and protein levels of Cth1 were clearly increased in the *msf1* mutant compared with the wild type. This is in line with the interaction between Msf1 and Cth1 indicated by 2D BN/SDS-PAGE and Y2H experiments (Figs. 5 and 6A; Supplemental Table S1) and indicates that the loss of Msf1 may trigger a compensatory response for chlorophyll synthesis in *Chlamydomonas*.

To determine the interrelation of Msf1 with chlorophyll in vivo, we performed greening experiments using the yellow in the dark mutants (Msf1-GFP5-1 and Msf1-GFP7-1). These mutants were obtained from the UVM4 transformants Msf1-GFP5 and Msf1-GFP7, respectively, in which these chimeric genes are driven by the authentic Msf1 promoter. The mutants were isolated by screening dark-grown cells for a yellow phenotype, indicating their inability to synthesize chlorophyll in the dark. However, in the light, these mutants turned green and accumulated normal levels of chlorophyll. Msf1-GFP5-1 and Msf1-GFP7-1 strains are only able to synthesize chlorophyll in the light, and thylakoid biogenesis can be induced by transferring dark-grown cultures to the light (Ohad et al., 1967; Malnoë et al., 1988; Falcioratore et al., 2005). Indeed, after 5 d of dark growth, the yellow mutants (Msf1-GFP5-1 and Msf1-GFP7-1) contained only trace amounts of chlorophyll (Fig. 7A). Chlorophyll synthesis resumed upon transfer to the light, and chlorophyll levels increased steadily during the greening period. Immunoblot analysis revealed that Msf1 was undetectable after 5 d of dark growth and accumulated concomitantly with chlorophyll upon exposure to light (Fig. 7B). A similar trend was observed in the wild-type strains Msf1-GFP5 and Msf1-GFP7. Although these strains are able to synthesize chlorophyll in the dark, they still increase their chlorophyll level in the light phase (Fig. 7B). Together with the known sequence of Msf1, which reveals the presence of several chlorophyll-binding sites (Fig. 4A), our results showing that there is a concomitant increase of Msf1 and chlorophyll during the development of thylakoid membranes strongly suggest that the binding of chlorophyll is required to stabilize Msf1. The same features have been observed for most LHC and chlorophyll-binding reaction center proteins (Dall’Osto et al., 2015).

Msf1 Is Induced under Specific Stress Conditions

To obtain more insights into the physiological role of Msf1, we performed several stress experiments. Considering that PSI contains more chlorophylls than PSII and that the insertion of chlorophyll into the PSI complex could be hindered under elevated temperature, we first examined the accumulation of PsA in the wild type (CC400) and *msf1* in response to heat stress (42°C). As shown in Figure 8A, the decrease of PsA in *msf1* was remarkably faster than in the wild type. Moreover, such a decrease was not observed in the complemented strains (C-23 and C-36), indicating that the maintenance of PSI under elevated temperature was severely

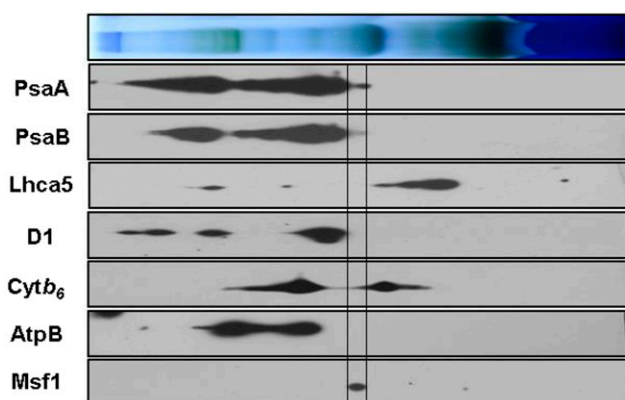


Figure 5. Separation of a novel thylakoid membrane complex containing Msf1 by 2D BN/SDS-PAGE and immunoblot analysis. Membrane proteins (equivalent to 10 μ g of chlorophyll) were solubilized with 2% β -dodecyl maltoside and then subjected to 2D BN/SDS-PAGE followed by immunoblotting using antibodies against the indicated proteins. The position of the complex containing Msf1 is indicated.

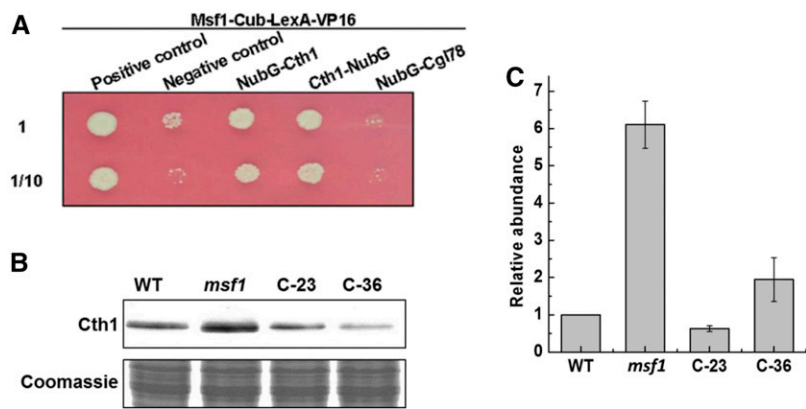


Figure 6. Interaction of Msf1 with Cth1. A, Split ubiquitin-based Y2H assay of Msf1 interaction with Cth1 (NubG-Cth1 and Cth1-NubG). Interactions were monitored by growth of serial 10-fold dilutions of yeast cells containing the indicated constructs on synthetic dextrose/-His/-Leu/-Trp/-Ade selection medium supplemented with 5 mM 3-amino-1,2,4-triazole. Positive and negative controls are NMY32-containing Cub-LexA-VP16-Msf1 transformed with the expression plasmid of NubI-Alg5 and NubG-Alg5, respectively. B, Immunoblot detection of Cth1 in the wild type (WT; CC400), *msf1*, and the complemented strains (C-23 and C-36). Membrane proteins (15 μ g per lane) were separated by 12% SDS-PAGE followed by immunoblot detection. Similar results were obtained in at least three independent experiments. C, qRT-PCR analysis of mRNA levels of Cth1 in the wild type (CC400), *msf1*, and the complemented strains (C-23 and C-36). sd values were estimated from three biological replicates each with two technical replicates ($n = 6$). Similar results were obtained in at least three independent experiments. The CBLP gene was used as a control.

compromised due to the loss of Msf1. The role of Msf1 during heat shock was further confirmed by examining the strains Msf1-GFP5 and Msf1-GFP7 (Fig. 8B). A marked increase in the level of Msf1 was detected upon exposure of these strains to the heat shock for 1 h, and the high level was maintained throughout the heat treatment. From

these results, we conclude that Msf1 plays a crucial role in protecting PSI and chlorophyll-binding proteins at elevated temperature.

Because PSI contains three 4Fe-4S clusters and represents an important iron sink in chloroplasts (Blaby-Haas and Merchant, 2013), we also investigated the accumulation of

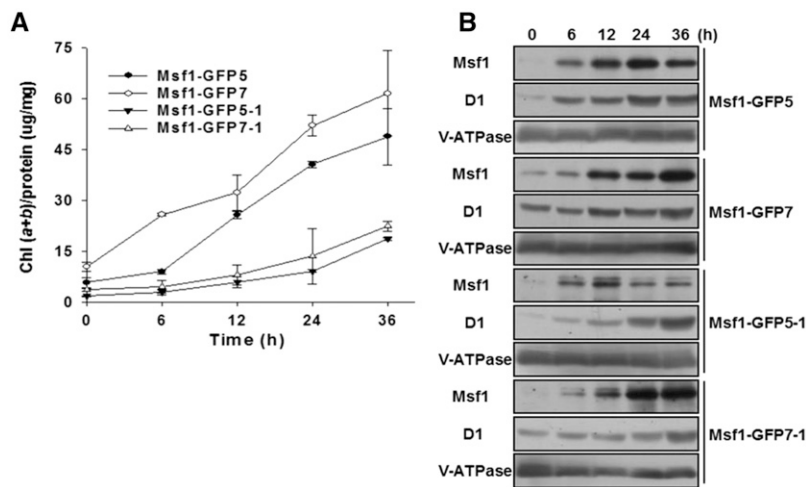


Figure 7. Msf1 accumulates concomitantly with chlorophyll during the greening of *Chlamydomonas*. A, Changes in chlorophyll content of the indicated strains. Cells grown for 5 d in the dark were transferred to the light. Cells were collected at five time points (from 0 to 36 h) in the light phase. Msf1-GFP5 and Msf1-GFP7 are two independent transformants capable of synthesizing chlorophyll in the dark. Msf1-GFP5-1 and Msf1-GFP7-1 are yellow in the dark mutants (unable to synthesize chlorophyll in the dark) derived from Msf1-GFP5 and Msf1-GFP7, respectively. sd values were estimated from three biological replicates each with three technical replicates. B, Changes in protein levels of the indicated strains detected by immunoblot analysis. Cells were grown and collected at different time points, as in A. Total protein extracted from each strain was separated by 12% SDS-PAGE (15 μ g per lane) followed by immunoblotting. V-ATPase was used as a loading control. The experiment was repeated more than three times, and similar results were obtained.

PSI key subunits (PsaA, PsaB, and PsaF) in the wild type, *msf1*, and the complemented strains (C-23 and C-36) in response to iron deficiency (Fig. 9). Since repression of cell growth was detectable after 12 h of iron deficiency (Zhao et al., 2013), samples were taken at 3, 6, and 12 h for immunoblot analysis (Fig. 9A). The data show that the decrease of core subunits of PSI in *msf1* was clearly faster than in the wild type, indicating that the maintenance of PSI under iron deficiency was severely compromised due to the loss of Msf1. This role of Msf1 under iron deficiency was further confirmed by examining Msf1 levels in the Msf1-GFP5 and Msf1-GFP7 strains (Fig. 9B). As expected, the accumulation of Msf1 in the Msf1-GFP5 and Msf1-GFP7 strains also increased during the 12-h stress treatment. Based on these data, we propose that the increase of Msf1 is part of a compensatory response for the maintenance of PSI during iron starvation.

Moreover, we investigated the accumulation of PSI key subunits (PsaA, PsaB, and PsaF) in the wild type, *msf1*, and the complemented strains (C-23 and C-36) under copper limitation. As shown in Figure 9, the decrease of the PSI core subunits in *msf1* was remarkably faster than in the wild type, indicating that the maintenance of PSI under copper limitation also was compromised in the mutant lacking Msf1. Earlier experiments by Moseley et al. (2002b) showed that, under copper deficiency, Cth1 is replaced by its isoenzyme Crd1 (Copper response defect1), and this has been suggested to be an essential step for PSI and LHCI maintenance. To further confirm the role of Msf1 under copper limitation, we then examined Msf1 levels in the Msf1-GFP5 and Msf1-GFP7 strains under this condition (Fig. 9B). As expected, a clear accumulation of Msf1 was observed in the strains under the stress condition. Compared with the level of Lhca5, which is relatively constant, the amount of Msf1 was increased significantly upon subjecting the cells to copper deprivation for 3 h, and it remained high afterward (6 and 12 h). Thus, these results strongly indicate that Msf1 functions in PSI and LHCI maintenance.

To further confirm that Msf1 functions toward the stability/maintenance of PSI, we monitored its accumulation in young and aging cells. Samples were taken from

liquid cultures over a range of cell densities (from 1×10^5 to 1×10^7 mL⁻¹) followed by immunoblot analysis (Fig. 9C). As expected, Msf1 was increased significantly as the cell concentration increased, and its highest level was observed in cells at the stationary phase (1×10^7 mL⁻¹). Since PSI contains more chlorophyll molecules than PSII and chlorophyll degradation is known to be enhanced during senescence, our data showing an increased level of Msf1 in aging cells further support the idea that this protein plays a crucial role in the maintenance of PSI. We presume that a substantial amount of Msf1 is required to maintain PSI and the chlorophyll-binding proteins in aging cells, probably to replace damaged chlorophyll molecules during this process.

DISCUSSION

In this work, we have identified Msf1 through a screen for mutants impaired in photosynthetic activity. A striking result of this study is that, although Msf1 is a member of the LHC-like protein superfamily, its expression is not stimulated by high-light stress and its abundance increases remarkably under specific stress conditions and in aging cells. We found that Msf1 is required for the accumulation and maintenance of protein-chlorophyll complexes, a feature that is especially pronounced for PSI. Interestingly, the protein appears to be linked to the chlorophyll biosynthetic pathway in *Chlamydomonas*. We propose that Msf1 represents a potential candidate for linking chlorophyll biosynthesis and the assembly/repair of chlorophyll-protein complexes, in particular in the case of PSI.

Msf1 Is Required for the Accumulation of Several Chlorophyll-Protein Complexes and the Maintenance of PSI

In the genome of *Chlamydomonas*, Msf1 is annotated as a hypothetical protein (Augustus 10.2; <http://augustus.gobics.de/predictions/chlamydomonas/>) with unknown function. Using a forward genetics approach, we have determined its important role in the maintenance of PSI and chlorophyll-binding proteins. This is based on the following observations. First, loss of Msf1 protein leads to

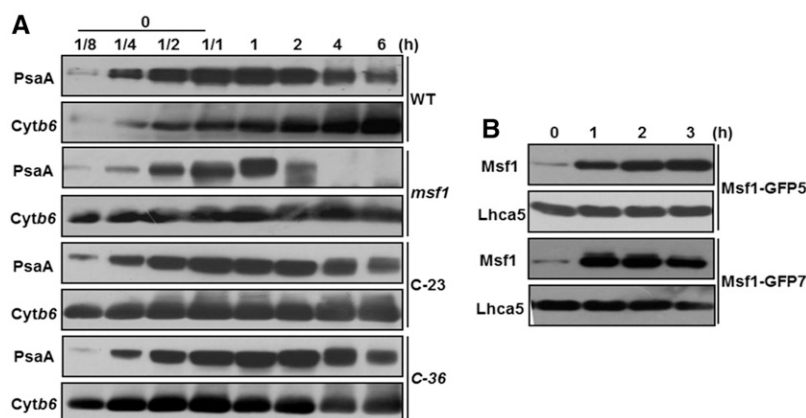


Figure 8. Immunoblot detection of PsaA and Msf1 under the heat shock stress condition. A, Levels of PsaA in the wild type (CC400), *msf1*, and the complemented strains (C-23 and C-36). B, Levels of Msf1 in Msf1-GFP strains (Msf1-GFP5 and Msf1-GFP7). Cells in the exponential growth phase at normal temperature (25°C) were shifted to elevated temperature (42°C) followed by sampling at five time points (from 0 to 6 h). Total proteins were separated by 12% SDS-PAGE (15 μ g per lane) followed by immunoblotting. Cytb6 was used as a loading control. In A, a four-serial dilution of protein extracts was used to quantify the immunosignals of the indicated proteins. Similar results were obtained in at least three biological replicates.

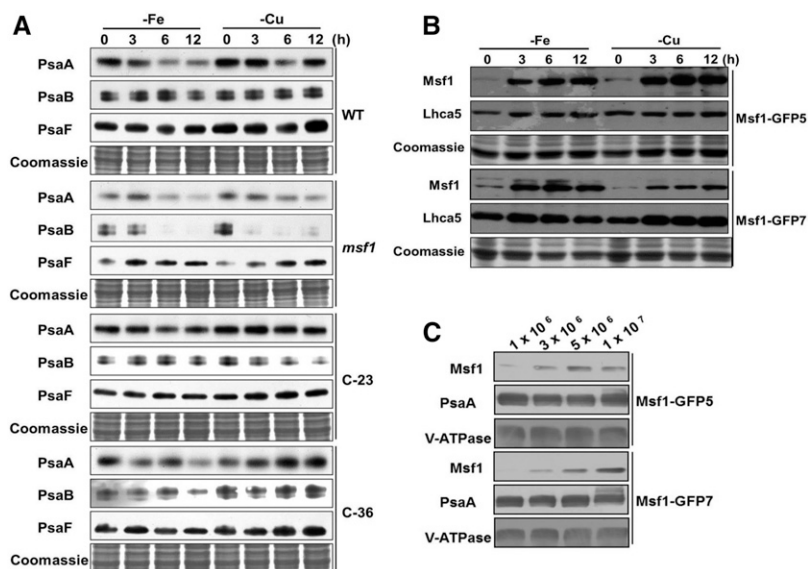


Figure 9. Immunoblot detection of PSI key subunits and Msf1 under iron and copper starvation and during aging of *Chlamydomonas*. A, Levels of PSI key subunits (PsaA, PsaB, and PsaF) in the wild type (WT; CC400), *msf1*, and the complemented strains (C-23 and C-36). B, Levels of Msf1 in Msf1-GFP strains (Msf1-GFP5 and Msf1-GFP7). In A and B, cells in the exponential growth phase were transferred to TAP (–Fe or –Cu) to achieve the stress treatment, respectively. Total proteins extracted from the cells collected at four time points were separated by 12% SDS-PAGE (15 μ g per lane) followed by immunoblotting. Lhca5 was used as a loading control. The experiment was repeated more than three times, and similar results were obtained. C, Levels of Msf1 in Msf1-GFP strains (Msf1-GFP5 and Msf1-GFP7) at different cell concentrations. Total proteins extracted from the cells collected at four cell concentrations were separated by 12% SDS-PAGE (15 μ g per lane) followed by immunoblotting. V-ATPase was used as a loading control. The experiment was repeated more than three times, and similar results were obtained.

a 4- to 5-fold decrease in abundance of the PSI reaction center proteins, with no or only minor effects on the levels of the other photosynthetic complexes (Fig. 2). Second, loss of Msf1 reduces the half-life/stability of PSI core proteins (PsaA and PsaD) but not that of PSII (D1; Fig. 3). Third, Msf1 accumulates to higher levels under stress conditions, some of which are known to preferentially affect PSI (heat shock and iron and copper limitation) and in aging cells (Fig. 7).

Unlike the known genes encoding PSI assembly or stability factors (Yang et al., 2015), *Msf1* encodes an LHC-like protein with predicted chlorophyll-binding sites. Genes encoding LHC-like proteins are ubiquitous in photosynthetic organisms. These proteins could be structurally attributed to four subfamilies (OHPs, SEPs, ELIPs, and PsbS) based on the number of transmembrane domains (Hedddad and Adamska, 2002; Komenda and Sobotka, 2016). Functional characterization using genetic and biochemical means has revealed distinct role(s) for individual proteins within or among these different subfamilies (Niyogi and Truong, 2013; Dinc et al., 2016; Beck et al., 2017). Msf1 resembles structurally LHC-like proteins containing three transmembrane domains (Fig. 4A), such as ELIPs, but is functionally distinct from them. Our finding that no increase in the transcript level of *Msf1* occurs under high light stress (Supplemental Fig. S5) clearly indicates that the regulation of this factor is different from that of known ELIPs (Hedddad and Adamska, 2002). Indeed, the abundance of Msf1 increases under heat

stress and iron and copper deficiency (Figs. 8 and 9), suggesting that it plays important roles in *Chlamydomonas* subjected to these stress conditions. The accumulation of high amounts of Msf1 in stationary phase cells (Fig. 9C) further suggests that this factor plays an important role for PSI maintenance. To the best of our knowledge, Msf1 represents the first LHC-like protein with three transmembrane domains required for the maintenance of PSI and of chlorophyll-binding proteins in *Chlamydomonas*.

Msf1 Is an LHC-Like Protein Linked to the Chlorophyll Biosynthetic Pathway

As described above, the Msf1 protein contains three predicted transmembrane domains and several putative chlorophyll-binding sites, a hallmark of LHC proteins, and is likely to adopt the same configuration as LHC proteins with the N-terminal domain on the stromal side of the thylakoid membrane. In contrast to most LHC proteins, Msf1 is a low-abundance protein. It also is present in several algae and plants, as revealed by BLAST search (<http://web.expasy.org/blast/>; data not shown), suggesting that Msf1 may have an important function in photosynthetic eukaryotes. Some of these proteins have been annotated as ELIPs or as carotene biosynthesis-related proteins. Whether these proteins act in a similar way to Msf1 remains to be determined.

Although several LHC-like proteins have been identified, little is known about their pigment-binding properties.

This is most likely due to the presence of numerous Lhc-like proteins with similar physicochemical properties *in vivo* and their transient expression, making the isolation and characterization of these proteins challenging (Bonente et al., 2011). In spite of several attempts, we were not able to reconstitute conclusively an Msf1 pigment-protein complex. Considering that earlier trials to reconstitute ELIP-like protein-pigment complexes (Tzvetkova-Chevolleau et al., 2007) also failed, it is possible that the binding of chlorophyll to these proteins is weak (R. Bassi, unpublished data).

It is known that pigments are required for the stability of most chlorophyll-binding LHC proteins. Here, we found that, as expected, Msf1 was undetectable in the yellow mutants (Msf1-GFP5-1 and Msf1-GFP7-1) grown in the dark, where they fail to accumulate chlorophyll. However, upon exposure to light, the level of Msf1 increased concomitantly with chlorophyll (Fig. 6, A and B). Also, an increase of Msf1 occurred in their wild-type progenitor strains (Msf1-GFP5 and Msf1-GFP7) upon a shift from the dark to the light, when chlorophyll synthesis is greatly enhanced (Fig. 6, A and B). These results are compatible with the ideas that this protein binds chlorophyll and that pigments are required for its stability, as is the case for most pigment-binding LHC proteins.

Interestingly, we found that Msf1 appears to be linked to the tetrapyrrole pathway. It interacts directly with Cth1 (CHL27B), as demonstrated in the Y2H assays, and cofractionates with Cth1 and Cgl78 in a 150-kD complex upon 2D BN/SDS-PAGE (Figs. 5 and 6A). Cth1 is a component of the aerobic chlorophyll cyclase, which catalyzes protochlorophyllide synthesis, one of the last steps of chlorophyll synthesis (Totter et al., 2003), and Cgl78 is involved in the regulation of the chlorophyll cyclase (Albus et al., 2012; Hollingshead et al., 2012). Cth1 has overlapping functions with Crd1, a paralogous protein required for PSI and LHCI maintenance under copper deficiency and anoxia, whereas Cth1 functions under copper-replete conditions (Moseley et al., 2000, 2002b). Our finding that Msf1 interacts with Cth1 suggests the existence of a possible link between chlorophyll synthesis and the assembly of pigment-protein complexes through Msf1. Because a marked decrease in the level of PSI reaction center proteins and several Lhca and Lhcb proteins, including CP29, was observed in the *msf1* mutant (Fig. 2), we propose that Msf1 may transiently store and/or transfer newly synthesized chlorophyll to these proteins and also may be involved in the chlorophyll assembly/association process of chlorophyll-binding proteins of PSI. Given the fact that, among the photosynthetic complexes, PSI binds the largest number of chlorophyll molecules, which are inserted in a coordinated way in its reaction center during its biogenesis, it is not surprising that factors have evolved for this task.

In cyanobacteria, Scp proteins, small chlorophyll *a/b* binding-like proteins, exist that contain one transmembrane domain related to the first and third transmembrane helices and the chlorophyll-binding sites of LHCI proteins (Heddad and Adamska, 2002; Komenda and Sobotka, 2016). It has been proposed that Scp proteins

function as chlorophyll-carrier proteins, and the binding of chlorophyll to these proteins has indeed been demonstrated in cyanobacteria (Storm et al., 2008). These proteins also have been proposed to be involved in the PSII repair cycle by serving as a temporary pigment reservoir with a low affinity for pigments when PSII components are being replaced (Promnares et al., 2006; Yao et al., 2007; Chidgey et al., 2014; Knoppová et al., 2014; Komenda and Sobotka, 2016). Scps appear to prevent the degradation of chlorophylls associated with PSII and could be involved in chlorophyll reutilization upon the repair of photo-damaged PSII (Vavilin et al., 2007). A link between chlorophyll biosynthesis and the cotranslational insertion of PSII reaction center proteins also is suggested by the isolation of a cyanobacterial protein complex comprising chlorophyll synthase and the high-light-inducible protein HliD together with the PSII assembly factor Ycf39, the YidC/Alb3 insertase, chlorophyllide, and carotenoids (Chidgey et al., 2014; Knoppová et al., 2014). These proteins are not associated exclusively with PSII, as they also have been found to interact with trimers of PSI in cyanobacteria (Wang et al., 2008; Akulinkina et al., 2015). Thus, we suggest that some of the functions ascribed to the Scps could be tailored for Msf1 in the maintenance of PSI and chlorophyll-binding proteins during evolution.

Msf1 Is an LHC-Like Protein Induced under Heat Stress and Nutrient Deficiency

The strongest response of Msf1 was observed under heat shock rather than under high-light stress (Fig. 8; Supplemental Fig. S5). In line with the above-proposed Msf1 function, the maintenance of PSI and chlorophyll-binding proteins may be compromised at elevated temperature and may require increased amounts of Msf1. Both iron and copper limitation lead to significant increases of Msf1, suggesting that this protein also may play crucial roles in these nutrient stress responses (Fig. 9). Iron starvation impacts PSI biogenesis, because this complex contains three 4Fe-4S clusters and represents an important iron sink in chloroplasts (Moseley et al., 2002a). It is thus possible that the observed increase of Msf1 is part of a compensatory response for alleviating the decrease of PSI under iron deficiency. The increase of Msf1 under copper deficiency is of particular interest with regard to the interaction between Msf1 and Cth1, a component of the aerobic oxidative cyclase that acts in the chlorophyll branch of the tetrapyrrole biosynthetic pathway (Moseley et al., 2002b; Totter et al., 2003). Our finding that this increase (Fig. 9) occurs when Cth1 is replaced by Crd1 under copper depletion could be linked to its proposed role in coordinating the synthesis of chlorophyll during the repair of chlorophyll-protein complexes.

CONCLUSION

The picture that emerges from this study is that Msf1 is up-regulated under a variety of stress conditions, including elevated temperature, deprivation of copper

and iron, and cell aging. The loss of Msf1 impacts the maintenance of PSI and several chlorophyll-binding proteins. Its interactions with components of the tetrapyrrole biosynthetic pathway and its ability to bind chlorophyll weakly suggest a role of Msf1 in coordinating chlorophyll synthesis with the maintenance of chlorophyll-protein complexes. Such a role may be particularly important for the maintenance of PSI and other chlorophyll-protein complexes under specific stress conditions to prevent the escape of free chlorophyll, which would cause photooxidative damage in the organism. Whether the homologous proteins present in several algae and higher plants act in a similar way to Msf1 remains to be determined.

MATERIALS AND METHODS

Strains, Culture Conditions, and Stress Treatments

Chlamydomonas reinhardtii wild-type strain CC400 (*mt+*) was obtained from the *Chlamydomonas* Genetics Center (www.chlamy.org), and UVM4 was obtained from Ralph Bock (Neupert et al., 2009). The *msf1* mutant was isolated from the insertion mutant library constructed in this work. For normal growth conditions, algal cells were cultured in TAP medium (Gorman and Levine, 1966) at 25°C under 60 $\mu\text{mol photons m}^{-2} \text{s}^{-1}$ continuous cool-white fluorescent light. For all experiments, cells were grown to midexponential phase and harvested by centrifugation, and the cell density was adjusted to 2 to 4×10^6 cells mL^{-1} . Growth tests on 1.5% agar plates (TAP and HSM) were performed by spotting 3 μL of serial dilutions of cells (from 2 to 4×10^6 cells mL^{-1}) and grown for several days. For stress treatments, high-light irradiance ($1,300 \mu\text{mol photons m}^{-2} \text{s}^{-1}$) and iron depletion were performed as described previously by Zhao et al. (2013). Heat shock and copper depletion were performed by following the descriptions by Mühlhaus et al. (2011) and Moseley et al. (2002b), respectively. For protein and mRNA analysis, cells were harvested at different time points by centrifugation at 2,500g and 4°C for 5 min. Cell pellets were washed once with 0.01 M sodium phosphate buffer (pH 7.4) and stored at -70°C .

Mutant Library Construction and Screening with Chlorophyll Fluorescence

The library of insertion mutants was constructed by transformation of the wild type (CC400) using the glass bead method with *KpnI*-linearized plasmid pSI103 containing the *aphVIII* gene conferring paromomycin resistance (Kindle, 1990). Transformants growing on TAP plates with 10 $\mu\text{g mL}^{-1}$ paromomycin (Sigma) were isolated and screened for mutants with reduced photosynthetic activity based on chlorophyll fluorescence measurements using the Maxi-Imaging PAM chlorophyll fluorometer (Walz) following the manufacturer's instructions. Sample preparation was done as described previously (Zhao et al., 2013), and the measurements were taken following the manufacturer's instructions. Among the mutants with the lowest ΦII values, *msf1* was chosen for subsequent characterization. 77K fluorescence emission spectra were measured using a fluorescence spectrophotometer (F-2500; Hitachi) as described (Yang et al., 2014) with slight modifications. An excitation wavelength of 435 nm (5-nm bandwidth) was used to induce chlorophyll fluorescence. The emission spectra were recorded in the range of 600 to 750 nm. The spectra were normalized according to Pinnola et al. (2015) with GFP as a fluorescence marker at 513 nm.

Pigment Analysis by HPLC

Pigment content from the wild type, *msf1*, and the complemented strains was determined by HPLC according to Thayer and Björkman (1990). Briefly, pigments from cells in exponential growth were extracted in acetone by vortexing for 1 min. After a short centrifugation, the supernatant was filtered through a 0.45- μm membrane filter and subsequently subjected to HPLC using the Waters system. Pigments from the reconstituted Msf1-pigment complex were extracted in 85% acetone buffered with Na_2CO_3 and then separated and quantified by HPLC as described (Gilmore and Yamamoto, 1991).

Protein Extraction, SDS-PAGE, and Immunoblot Analysis

Total protein extraction from *Chlamydomonas*, separation by SDS-PAGE (12% polyacrylamide), and immunoblot analysis were done as described (Zhao et al., 2013). The *Chlamydomonas* antibodies against D1, D2, CP43, CP47, *Cytb_f*, *AtpB*, V-ATPase, and *Cth1* were from Agrisera and diluted according to the supplier's instructions. The GFP antibody was from Beijing TransGen Biotech and used with a dilution of 1:1,000. Antibodies against PsaA, PsaB, PsaC, PsaD, PsaF, Lhca1/3/4/5/6/7/8/9, Ycf3, Ycf4, CP29, and LhcII were from J.-D. Rochaix (University of Geneva). The blots were scanned using a UMAX Power-Look 2100XL scanner (Willich). Protein content was determined by the method of Bradford (1976) using BSA as a standard.

2D BN/SDS-PAGE and Protein Detection

2D BN/SDS-PAGE of membrane protein complexes was performed according to Yang et al. (2014), except that the glass bead lysis method was used for the isolation of membrane proteins according to Göhre et al. (2006). After separation in the second dimension, the gel was used for immunoblot analysis as described above.

Genetic Analysis

For DNA-blot analysis, genomic DNA was isolated from the wild type and the *msf1* mutant using the Plant Genomic DNA Kit according to the manufacturer's instructions (Tiagen Biotech). Approximately 10 μg of genomic DNA was digested overnight with the restriction endonucleases *Bam*HI and *Hind*III (New England Biolabs). The fragments resulting from the digestion were separated by agarose (0.8%) gel electrophoresis, blotted onto nitrocellulose membranes, and hybridized according to the manufacturer's instructions with the DIG High Prime DNA Labeling and Detection Starter Kit II from Roche (catalog no. 11585614910). The detection was performed using CSPD for chemiluminescence (Roche).

For gene mapping, genomic DNA flanking the *aphVIII* gene was isolated using high-efficiency thermal asymmetric intercalated PCR with the specific primers listed in Supplemental Table S2 according to Liu and Chen (2007) with modifications. The primary amplification reactions (20 μL) contained 2 μL of PCR buffer (Takara Bio), 200 μM deoxyribonucleotide triphosphates (Beijing TransGen Biotech), 1 μM of any of the LAD primers, 0.3 μM SP0, 0.5 μL of LA Taq (Takara Bio), and 20 to 30 ng of DNA. Each 25- μL secondary reaction contained 2.5 μL of PCR buffer, 200 μM each of deoxyribonucleotide triphosphates, 0.3 μM AC1 and SP1, 0.5 μL of LA Taq, and 1 μL of 50-fold diluted primary product. The amplified products from the secondary reactions were analyzed by agarose gel electrophoresis and were purified prior to sequencing. Sequencing reactions were performed by Beijing Sunbiotech, and the sequence data were used to search the *Chlamydomonas* genome. For tetrad analysis, genetic crosses between *msf1* and the wild type and zygote dissection were performed as described (Harris, 1989). The mutant was backcrossed twice, and four progeny from distinct zygotes of the second generation (*T2-msf1*) were obtained.

Plasmid Construction

To complement the *msf1* mutant, the gene was amplified from the wild type (CC400) with primers listed in Supplemental Table S2. The amplification product was then digested with *Nde*I and *Eco*RI and subcloned into the similarly treated vector pJR38 (Neupert et al., 2009). The constructed plasmids were introduced into *msf1* mutant cells by transformation, and the transformants were analyzed subsequently by chlorophyll fluorescence measurements. Colonies displaying a wild-type phenotype also were analyzed for the integration of *Msf1* by PCR with primers listed in Supplemental Table S2.

To construct the GFP fusion vector for subcellular localization analysis, the GFP-coding sequence (with pJR38 as template) was amplified with primers listed in Supplemental Table S2, with *Eco*RI restriction sites at both sites. After excision, *Msf1* cDNA (*Nde*I/*Eco*RI) and GFP (*Eco*RI/*Eco*RI) were ligated into the plasmid pDBle, generating vector pDBle-Msf1-GFP. After verification by sequencing, the plasmid was transformed into the UVM4 strain using the glass bead method.

Protein Identification by LC-MS/MS

To identify proteins in the Msf1 complex, the band containing the complex was excised and analyzed by LC-MS/MS. In-gel digestion was performed as

described (Wang et al., 2000; Huang et al., 2002) with modifications according to Fandiño et al., (2005). Briefly, the gel band was cut into 1- to 2-mm² pieces and then dehydrated with a small volume of acetonitrile for 10 min. The gel pieces were then freeze dried by SpeedVac followed by incubation in 100 μ L of 8 M urea for denaturation (30 min). Prior to reduction and alkylation, the gel slices were destained with a buffer containing 25 mM ammonium bicarbonate and 50% acetonitrile and dried. The proteins in the gel slices were then sequentially reduced and alkylated with 10 mM DTT and 55 mM iodoacetamide, respectively, followed by digestion with trypsin (Sigma) at 37°C overnight. The tryptic peptides were extracted from the gel with a buffer containing 5% trifluoroacetic acid and 50% acetonitrile and then freeze dried by SpeedVac. The peptides were resolubilized in 0.1% formic acid and filtered with a 0.45- μ m centrifugal filter before liquid chromatography-mass spectrometry analysis. The peptides were analyzed with a TripleTOF5600 mass spectrometer (ABSciex) coupled online to an Eksigent nanoLC Ultra device. The liquid chromatography gradient contained buffer A (0.1% formic acid in water) and buffer B (0.1% formic acid in acetonitrile) and was increased linearly from 5% to 90% B for 90 min with a 300 nL min⁻¹ flow rate. The peptides were identified by searching the tandem mass spectrometry spectra against the *Chlamydomonas* proteome sequence database (downloaded from SwissProt) using ProteinPilot software 4.2. Carbamidomethylation of Cys residues was included as the fixed modification. The mass tolerance was set to 0.05 D, and a maximum of two missed cleavages was allowed. The false discovery rate was set at 1% for both protein and peptide identification.

Split Ubiquitin-Based Y2H Assays and qRT-PCR Analysis

Protein-protein interactions were detected by split ubiquitin-based Y2H assays using the yeast strain NMY32 supplied by Dualsystems Biotech. The pNCW vector was used to construct the bait plasmids, and the prey plasmids were constructed from the vector pDSL_{Nx} or pDSL_{2xN}, which encodes the NubG fragment (Dualsystems Biotech). Primers used for plasmid construction for the yeast assay are listed in Supplemental Table S2, and *Sfi*I sites were added to both primers. Interactions were monitored by growth of 10-fold serially diluted yeast cells containing the indicated constructs on SD/-His/-Leu/-Trp/-Ade selection medium supplemented with 5 mM 3-amino-1,2,4-triazole. Positive and negative controls were NMY32-containing Cub-LexA-VP16-Msf1 transformed with the expression plasmid of Nub1-Alg5 and NubG-Alg5, respectively. Quantitative real-time reverse transcription-PCR was performed as described previously (Zhao et al., 2013) with *CBLP* as the internal control. Gene-specific PCR primer pairs for *Chl1*, *Msf1*, *LhcSR3.1*, and *ELI2-1* were designed using Primer3 software (<http://frodo.wi.mit.edu/>) and are listed in Supplemental Table S2. Relative abundance was expressed as the fold change in expression level relative to the reference, calculated as $2^{-\Delta\Delta C_t}$.

Reconstitution of Msf1 and CP29 Pigment-Protein Complexes

Recombinant Msf1 and CP29 in inclusion bodies were purified from *Escherichia coli* (BL21 strain; Stratagene) transformed with either Msf1- or CP29-pQBH22. *E. coli* was grown in SB medium to OD = 0.25, and then protein expression was induced by adding 2 mM isopropylthio- β -galactoside. Bacterial cultures were grown for 6 h at 28°C under continuous stirring. Total pigments extracted from thylakoids of Arabidopsis (*Arabidopsis thaliana*) or reconstituted complexes were extracted with 80% acetone, and the concentrations were determined spectroscopically or by HPLC as described (Porra and Grimme, 1974). The procedure for the reconstitution trials mimicked that described for CP29 (Giuffra et al., 1996) with the following modifications: the chlorophyll:protein ratio in the reconstitution mixture was set to either 8 or 12, and the carotenoid:protein ratio was set to 5. The chlorophyll *a/b* ratio in the mixture was either 2.1 (for pigments isolated from wild-type thylakoids) or 3.1 (from *npq2* thylakoids). Reconstitution was achieved by two subsequent cycles of freezing (20 min, -20°C) and thawing (20 min, 0°C). One percent *n*-octyl β -D-glucopyranoside was then substituted for lithium dodecylsulfate by precipitation of the KDS (potassium dodecylsulfate) following the addition of 150 mM KCl, incubation for 15 min on ice, and centrifugation (10 min at 20,000g). The mixture was then loaded onto a 12-mL Suc gradient (0.1–1 M), containing 10 mM HEPES/KOH, pH 7.8, and 0.06% dodecyl β -D-maltoside, and centrifuged 24 h at 254,000g in a Beckman SW41 rotor. The lower green band (at about 0.4 M Suc) contained the reconstituted complex and was harvested with a syringe and subjected for further analysis.

Accession Numbers

Sequence data from this article can be found in the GenBank/EMBL data libraries under the following accession numbers: Msf1 (XP_001692700.1), Lhcbm1 (AAM18057.1), CP26 (XP_001695927.1), ELI1 (XP_001695978.1), CP29 (XP_001697193.1), and PsbS (XP_001689476.1) from *Chlamydomonas* and ELIP1 (P93735) from Arabidopsis.

Supplemental Data

The following supplemental materials are available.

Supplemental Figure S1. Identification and complementation of the *msf1* mutant.

Supplemental Figure S2. Transmission electron microscopy of cells from the wild type, *msf1*, and the complemented strains (C-23 and C-36).

Supplemental Figure S3. Analysis of recombinant Msf1 and sensitivity of the Msf1 antibodies.

Supplemental Figure S4. Complementation of the *msf1* mutant with the Msf1-GFP fusion construct.

Supplemental Figure S5. qRT-PCR analysis of the expression patterns of Msf1 in response to high-light stress (1,300 μ mol photons m⁻² s⁻¹).

Supplemental Table S1. Proteins of the Msf1 complex isolated by BN gel electrophoresis and identified by LC-MS/MS.

Supplemental Table S2. List of primers used in this study.

Supplemental Data Set S1. LC-MS/MS data in relation to Supplemental Table S1.

Received September 19, 2016; accepted June 20, 2017; published June 21, 2017.

LITERATURE CITED

- Adamska I (2001) The Elip family of stress proteins in the thylakoid membrane of pro- and eukaryota. *Adv Photosynth Respir* 11: 487–505
- Akulinkina DV, Bolychevtseva YV, Elanskaya IV, Karapetyan NV, Yurina NP (2015) Association of high light-inducible HliA/HliB stress proteins with photosystem 1 trimers and monomers of the cyanobacterium *Synechocystis* PCC 6803. *Biochemistry (Mosc)* 80: 1254–1261
- Albus CA, Salinas A, Czarnecki O, Kahla S, Rothbart M, Thiele W, Lein W, Bock R, Grimm B, Schöttler MA (2012) LCAA, a novel factor required for magnesium protoporphyrin monomethylester cyclase accumulation and feedback control of aminolevulinic acid biosynthesis in tobacco. *Plant Physiol* 160: 1923–1939
- Amunts A, Nelson N (2009) Plant photosystem I design in the light of evolution. *Structure* 17: 637–650
- Beck J, Lohscheider JN, Albert S, Andersson U, Mendgen KW, Rojas-Stütz MC, Adamska I, Funck D (2017) Small one-helix proteins are essential for photosynthesis in Arabidopsis. *Front Plant Sci* 8: 7
- Blaby-Haas CE, Merchant SS (2013) Iron sparing and recycling in a compartmentalized cell. *Curr Opin Microbiol* 16: 677–685
- Bonente G, Ballottari M, Truong TB, Morosinotto T, Ahn TK, Fleming GR, Niyogi KK, Bassi R (2011) Analysis of LhcSR3, a protein essential for feedback de-excitation in the green alga *Chlamydomonas reinhardtii*. *PLoS Biol* 9: e1000577
- Bonente G, Howes BD, Caffarri S, Smulevich G, Bassi R (2008) Interactions between the photosystem II subunit PsbS and xanthophylls studied *in vivo* and *in vitro*. *J Biol Chem* 283: 8434–8445
- Bradford MM (1976) A rapid and sensitive method for the quantitation of microgram quantities of protein utilizing the principle of protein-dye binding. *Anal Biochem* 72: 248–254
- Caffarri S, Passarini F, Bassi R, Croce R (2007) A specific binding site for neoxanthin in the monomeric antenna proteins CP26 and CP29 of photosystem II. *FEBS Lett* 581: 4704–4710
- Cammarata KV, Plumley FG, Schmidt GW (1992) Pigment and protein composition of reconstituted light-harvesting complexes and effects of some protein modifications. *Photosynth Res* 33: 235–250
- Cheregi O, Vermaas W, Funk C (2012) The search for new chlorophyll-binding proteins in the cyanobacterium *Synechocystis* sp. PCC 6803. *J Biotechnol* 162: 124–133

- Chidgey JW, Linhartová M, Komenda J, Jackson PJ, Dickman MJ, Canniffe DP, Koník P, Pilný J, Hunter CN, Sobotka R (2014) A cyanobacterial chlorophyll synthase-HliD complex associates with the Ycf39 protein and the YidC/Alb3 insertase. *Plant Cell* **26**: 1267–1279
- Dall'Osto L, Bressan M, Bassi R (2015) Biogenesis of light harvesting proteins. *Biochim Biophys Acta* **1847**: 861–871
- Dinc E, Tian L, Roy LM, Roth R, Goodenough U, Croce R (2016) LHCSR1 induces a fast and reversible pH-dependent fluorescence quenching in LHClI in *Chlamydomonas reinhardtii* cells. *Proc Natl Acad Sci USA* **113**: 7673–7678
- Dolganov NA, Bhaya D, Grossman AR (1995) Cyanobacterial protein with similarity to the chlorophyll a/b binding proteins of higher plants: evolution and regulation. *Proc Natl Acad Sci USA* **92**: 636–640
- Dominici P, Caffarri S, Armenante F, Ceoldo S, Crimi M, Bassi R (2002) Biochemical properties of the PsbS subunit of photosystem II either purified from chloroplast or recombinant. *J Biol Chem* **277**: 22750–22758
- Elrad D, Grossman AR (2004) A genome's-eye view of the light-harvesting polypeptides of *Chlamydomonas reinhardtii*. *Curr Genet* **45**: 61–75
- Falcatore A, Merendino L, Barneche F, Ceol M, Meskauskiene R, Apel K, Rochaix JD (2005) The FLP proteins act as regulators of chlorophyll synthesis in response to light and plastid signals in *Chlamydomonas*. *Genes Dev* **19**: 176–187
- Fandino AS, Rais I, Vollmer M, Elgass H, Schägger H, Karas M (2005) LC-nanospray-MS/MS analysis of hydrophobic proteins from membrane protein complexes isolated by blue-native electrophoresis. *J Mass Spectrom* **40**: 1223–1231
- Gilmore AM, Yamamoto HY (1991) Zeaxanthin formation and energy-dependent fluorescence quenching in pea chloroplasts under artificially mediated linear and cyclic electron transport. *Plant Physiol* **96**: 635–643
- Giuffra E, Cugini D, Croce R, Bassi R (1996) Reconstitution and pigment-binding properties of recombinant CP29. *Eur J Biochem* **238**: 112–120
- Göhre V, Ossenbühl F, Crèvecoeur M, Eichacker LA, Rochaix JD (2006) One of two alb3 proteins is essential for the assembly of the photosystems and for cell survival in *Chlamydomonas*. *Plant Cell* **18**: 1454–1466
- Gorman DS, Levine RP (1966) Cytochrome f and plastocyanin: their sequence in the photosynthetic electron transport chain of *Chlamydomonas reinhardtii*. *Proc Natl Acad Sci USA* **54**: 1665–1669
- Harris EH (1989) The *Chlamydomonas* Source Book: A Comprehensive Guide to Biology and Laboratory Use. Academic Press, San Diego
- Havaux M, Guedeney G, He Q, Grossman AR (2003) Elimination of high-light-inducible polypeptides related to eukaryotic chlorophyll a/b-binding proteins results in aberrant photoacclimation in *Synechocystis* PCC6803. *Biochim Biophys Acta* **1557**: 21–33
- Hedda M, Adamska I (2002) The evolution of light stress proteins in photosynthetic organisms. *Comp Funct Genomics* **3**: 504–510
- Hollingshead S, Kopecká J, Jackson PJ, Canniffe DP, Davison PA, Dickman MJ, Sobotka R, Hunter CN (2012) Conserved chloroplast open-reading frame ycf54 is required for activity of the magnesium protoporphyrin monomethyl ester oxidative cyclase in *Synechocystis* PCC 6803. *J Biol Chem* **287**: 27823–27833
- Hsieh SI, Castruita M, Malasarn D, Urzica E, Erde J, Page MD, Yamasaki H, Casero D, Pellegrini M, Merchant SS, et al (2013) The proteome of copper, iron, zinc, and manganese micronutrient deficiency in *Chlamydomonas reinhardtii*. *Mol Cell Proteomics* **12**: 65–86
- Huang F, Parmryd I, Nilsson F, Persson AL, Pakrasi HB, Andersson B, Norling B (2002) Proteomics of *Synechocystis* sp. strain PCC 6803: identification of plasma membrane proteins. *Mol Cell Proteomics* **1**: 956–966
- Hutin C, Nussaume L, Moise N, Moya I, Kloppstech K, Havaux M (2003) Early light-induced proteins protect Arabidopsis from photooxidative stress. *Proc Natl Acad Sci USA* **100**: 4921–4926
- Kim S, Sandusky P, Bowlby NR, Aebersold R, Green BR, Vlahakis S, Yocum CF, Pichersky E (1992) Characterization of a spinach psbS cDNA encoding the 22 kDa protein of photosystem II. *FEBS Lett* **314**: 67–71
- Kindle KL (1990) High-frequency nuclear transformation of *Chlamydomonas reinhardtii*. *Proc Natl Acad Sci USA* **87**: 1228–1232
- Knoppová J, Sobotka R, Tichý M, Yu J, Koník P, Halada P, Nixon PJ, Komenda J (2014) Discovery of a chlorophyll binding protein complex involved in the early steps of photosystem II assembly in *Synechocystis*. *Plant Cell* **26**: 1200–1212
- Komenda J, Sobotka R (2016) Cyanobacterial high-light-inducible proteins: protectors of chlorophyll-protein synthesis and assembly. *Biochim Biophys Acta* **1857**: 288–295
- Kufryk G, Hernandez-Prieto MA, Kieselbach T, Miranda H, Vermaas W, Funk C (2008) Association of small CAB-like proteins (SCPs) of *Synechocystis* sp. PCC 6803 with photosystem II. *Photosynth Res* **95**: 135–145
- Kühlbrandt W, Wang DN, Fujiyoshi Y (1994) Atomic model of plant light-harvesting complex by electron crystallography. *Nature* **367**: 614–621
- Liu YG, Chen Y (2007) High-efficiency thermal asymmetric interlaced PCR for amplification of unknown flanking sequences. *Biotechniques* **43**: 649–656
- Malnoë P, Mayfield SP, Rochaix JD (1988) Comparative analysis of the biogenesis of photosystem II in the wild-type and Y-1 mutant of *Chlamydomonas reinhardtii*. *J Cell Biol* **106**: 609–616
- Mazor Y, Borovikova A, Nelson N (2015) The structure of plant photosystem I super-complex at 2.8 Å resolution. *eLife* **4**: e07433
- Montané MH, Kloppstech K (2000) The family of light-harvesting-related proteins (LHCs, ELIPs, HLIPs): was the harvesting of light their primary function? *Gene* **258**: 1–8
- Moseley J, Quinn J, Eriksson M, Merchant S (2000) The Crd1 gene encodes a putative di-iron enzyme required for photosystem I accumulation in copper deficiency and hypoxia in *Chlamydomonas reinhardtii*. *EMBO J* **19**: 2139–2151
- Moseley JL, Allinger T, Herzog S, Hoerth P, Wehinger E, Merchant S, Hippler M (2002a) Adaptation to Fe-deficiency requires remodeling of the photosynthetic apparatus. *EMBO J* **21**: 6709–6720
- Moseley JL, Page MD, Alder NP, Eriksson M, Quinn J, Soto F, Theg SM, Hippler M, Merchant S (2002b) Reciprocal expression of two candidate di-iron enzymes affecting photosystem I and light-harvesting complex accumulation. *Plant Cell* **14**: 673–688
- Mühlhaus T, Weiss J, Hemme D, Sommer F, Schroda M (2011) Quantitative shotgun proteomics using a uniform ¹⁵N-labeled standard to monitor proteome dynamics in time course experiments reveals new insights into the heat stress response of *Chlamydomonas reinhardtii*. *Mol Cell Proteomics* **10**: M110.004739
- Nelson N (2009) Plant photosystem I: the most efficient nano-photochemical machine. *J Nanosci Nanotechnol* **9**: 1709–1713
- Neupert J, Karcher D, Bock R (2009) Generation of *Chlamydomonas* strains that efficiently express nuclear transgenes. *Plant J* **57**: 1140–1150
- Niyogi KK, Truong TB (2013) Evolution of flexible non-photochemical quenching mechanisms that regulate light harvesting in oxygenic photosynthesis. *Curr Opin Plant Biol* **16**: 307–314
- Ohad I, Siekevitz P, Palade GE (1967) Biogenesis of chloroplast membranes. I. Plastid dedifferentiation in a dark-grown algal mutant (*Chlamydomonas reinhardtii*). *J Cell Biol* **35**: 521–552
- Peers G, Truong TB, Ostendorf E, Busch A, Elrad D, Grossman AR, Hippler M, Niyogi KK (2009) An ancient light-harvesting protein is critical for the regulation of algal photosynthesis. *Nature* **462**: 518–521
- Pinnola A, Cazzaniga S, Alboresi A, Nevo R, Levin-Zaidman S, Reich Z, Bassi R (2015) Light-harvesting complex stress-related proteins catalyze excess energy dissipation in both photosystems of *Physcomitrella patens*. *Plant Cell* **27**: 3213–3227
- Porra RJ, Grimme LH (1974) A new procedure for the determination of chlorophylls a and b and its application to normal and regreening *Chlorella*. *Anal Biochem* **57**: 255–267
- Promnare K, Komenda J, Bumba L, Nebesarova J, Vacha F, Tichý M (2006) Cyanobacterial small chlorophyll-binding protein ScpD (HliB) is located on the periphery of photosystem II in the vicinity of PsbH and CP47 subunits. *J Biol Chem* **281**: 32705–32713
- Qin X, Suga M, Kuang T, Shen JR (2015) Photosynthesis: structural basis for energy transfer pathways in the plant PSI-LHCI supercomplex. *Science* **348**: 989–995
- Rahire M, Larocque F, Cerutti L, Rochaix JD (2012) Identification of an OPR protein involved in the translation initiation of the PsbA subunit of photosystem I. *Plant J* **72**: 652–661
- Scholes GD, Fleming GR, Olaya-Castro A, van Grondelle R (2011) Lessons from nature about solar light harvesting. *Nat Chem* **3**: 763–774
- Staleva H, Komenda J, Shukla MK, Šlouf V, Kaňa R, Polívka T, Sobotka R (2015) Mechanism of photoprotection in the cyanobacterial ancestor of plant antenna proteins. *Nat Chem Biol* **11**: 287–291
- Storm P, Hernandez-Prieto MA, Eggink LL, Hooper JK, Funk C (2008) The small CAB-like proteins of *Synechocystis* sp. PCC 6803 bind chlorophyll: *in vitro* pigment reconstitution studies on one-helix light-harvesting-like proteins. *Photosynth Res* **98**: 479–488
- Takahashi Y, Yasui TA, Stauber EJ, Hippler M (2004) Comparison of the subunit compositions of the PSI-LHCI supercomplex and the LHClI in the green alga *Chlamydomonas reinhardtii*. *Biochemistry* **43**: 7816–7823
- Teramoto H, Ishii A, Kimura Y, Hasegawa K, Nakazawa S, Nakamura T, Higashi S, Watanabe M, Ono TA (2006) Action spectrum for expression

- of the high intensity light-inducible Lhc-like gene Lhl4 in the green alga *Chlamydomonas reinhardtii*. *Plant Cell Physiol* **47**: 419–425
- Teramoto H, Itoh T, Ono TA** (2004) High-intensity-light-dependent and transient expression of new genes encoding distant relatives of light-harvesting chlorophyll-a/b proteins in *Chlamydomonas reinhardtii*. *Plant Cell Physiol* **45**: 1221–1232
- Thayer SS, Björkman O** (1990) Leaf xanthophyll content and composition in sun and shade determined by HPLC. *Photosynth Res* **23**: 331–343
- Totter S, Block MA, Allen M, Westergren T, Albrieux C, Scheller HV, Merchant S, Jensen PE** (2003) *Arabidopsis* CHL27, located in both envelope and thylakoid membranes, is required for the synthesis of protochlorophyllide. *Proc Natl Acad Sci USA* **100**: 16119–16124
- Tzvetkova-Chevolleau T, Franck F, Alawady AE, Dall'Osto L, Carrière F, Bassi R, Grimm B, Nussaume L, Havaux M** (2007) The light stress-induced protein ELIP2 is a regulator of chlorophyll synthesis in *Arabidopsis thaliana*. *Plant J* **50**: 795–809
- Vavilin D, Yao D, Vermaas W** (2007) Small Cab-like proteins retard degradation of photosystem II-associated chlorophyll in *Synechocystis* sp. PCC 6803: kinetic analysis of pigment labeling with ¹⁵N and ¹³C. *J Biol Chem* **282**: 37660–37668
- Wang Q, Jantaro S, Lu B, Majeed W, Bailey M, He Q** (2008) The high light-inducible polypeptides stabilize trimeric photosystem I complex under high light conditions in *Synechocystis* PCC 6803. *Plant Physiol* **147**: 1239–1250
- Wang Y, Sun J, Chitnis PR** (2000) Proteomic study of the peripheral proteins from thylakoid membranes of the cyanobacterium *Synechocystis* sp. PCC 6803. *Electrophoresis* **21**: 1746–1754
- Wollman FA, Bennoun P** (1982) A new protein chlorophyll complex related to photosystem I in *Chlamydomonas*. *Biochim Biophys Acta* **80**: 352–360
- Xu H, Vavilin D, Funk C, Vermaas W** (2002) Small Cab-like proteins regulating tetrapyrrole biosynthesis in the cyanobacterium *Synechocystis* sp. PCC 6803. *Plant Mol Biol* **49**: 149–160
- Xu H, Vavilin D, Funk C, Vermaas W** (2004) Multiple deletions of small Cab-like proteins in the cyanobacterium *Synechocystis* sp. PCC 6803: consequences for pigment biosynthesis and accumulation. *J Biol Chem* **279**: 27971–27979
- Yang H, Liao L, Bo T, Zhao L, Sun X, Lu X, Norling B, Huang F** (2014) Slr0151 in *Synechocystis* sp. PCC 6803 is required for efficient repair of photosystem II under high-light condition. *J Integr Plant Biol* **56**: 1136–1150
- Yang H, Liu J, Wen X, Lu C** (2015) Molecular mechanism of photosystem I assembly in oxygenic organisms. *Biochim Biophys Acta* **1847**: 838–848
- Yao D, Kieselbach T, Komenda J, Promnares K, Prieto MA, Tichy M, Vermaas W, Funk C** (2007) Localization of the small CAB-like proteins in photosystem II. *J Biol Chem* **282**: 267–276
- Zhao L, Chen M, Cheng D, Yang H, Sun Y, Zhou H, Huang F** (2013) Different B-type methionine sulfoxide reductases in *Chlamydomonas* may protect the alga against high-light, sulfur-depletion, or oxidative stress. *J Integr Plant Biol* **55**: 1054–1068